DETERMINATION OF THE CHROMATICITY OF THE TI 8 TRANSFER LINE BASED ON KICK RESPONSE MEASUREMENTS

K. Fuchsberger, S. Fartoukh, B. Goddard, R. Jones, V. Kain, M. Meddahi,
V. Mertens, J. Wenninger, CERN, Geneva, Switzerland

Abstract

The 3 km long TI 8 transfer line is used to transfer 450 GeV proton and ion beams from the SPS to LHC collider. As part of a detailed optics investigation program the chromaticity of the transfer line was measured. Kick response data of the transfer line was recorded for various extraction energy offsets in the SPS. The quadrupolar and sextupolar field errors (b_2 and b_3, respectively) over the whole transfer line dipoles, a systematic error of the main quadrupole strengths and the initial momentum error were estimated by a fit. Using the updated model, the chromaticity of the line was then calculated.

MEASUREMENTS

Kick response measurements in 2006 revealed a visible phase error in the vertical plane in the transfer line. By fitting the strengths of the two main quadrupole families a relatively large detuning (6.5 permill) of the main vertical focussing quadrupole strength was found, while the horizontal focussing quadrupole strength was in good consistency with the model (error of about 0.6 permill) [1]. Later, during the injection tests in 2008 [2], a strong dispersion mismatch with the onset around the junction between TI 8 and the LHC was observed, as shown in Fig. 1.

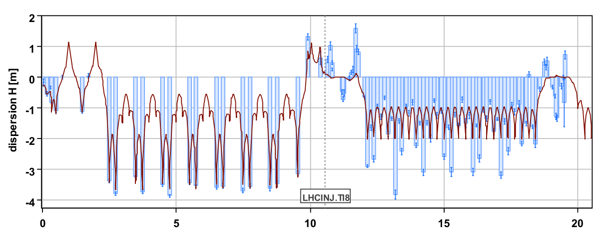

Figure 1: Horizontal dispersion of TI 8 and LHC sector 78. Bars represent the measured dispersion and the line represent the dispersion calculated from the nominal model.

Many possible sources for these inconsistencies were investigated [3]. As part of the TI 8 optics investigation program also the determination of the quadrupolar and sextupolar field errors of the main bends in the line was scheduled for further studies.

The measurement procedure consisted of recording kick-response data for 4 correctors in each plane. The correctors were excited by $\pm 40\,\mu\mathrm{rad}$ with respect to their nominal setting. The measurement was repeated for 7 different values of the initial energy offset $\frac{\delta p}{p}$ at the exit of the SPS (-2, -1, -0.5, 0.0, +0.5, +1 and +2 permill).

Already from the raw measurement data it is clear that the horizontal response depends strongly on $\frac{\delta p}{p}$ (Fig. 2), while the vertical response does not (Fig. 3).

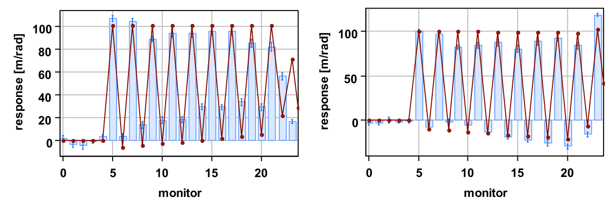

(a) $\frac{\delta p}{p} = -0.002$ (b) $\frac{\delta p}{p} = +0.002$

Figure 2: Horizontal response for one horizontal corrector. Bars represent the measured data, dots the nominal model. A clear dependence on $\frac{\delta p}{p}$ is visible, which is only partly reproduced by the model.

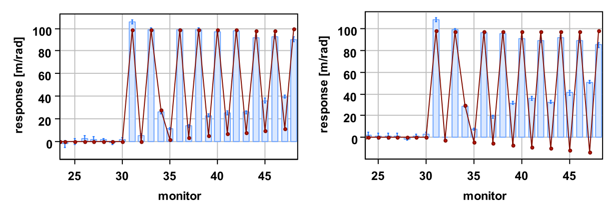

(a) $\frac{\delta p}{p} = -0.002$ (b) $\frac{\delta p}{p} = +0.002$

Figure 3: Vertical response for one vertical corrector. Bars represent the measured data, dots the nominal model. Almost no difference in the measured data is visible, while there should be a dependence on $\frac{\delta p}{p}$ according to the model.

ANALYSIS PRINCIPLE

The data analysis for this paper was done using the *Aloha (Another linear optics helper application)* software [4]. This software is a JAVA-reimplementation of the well known principle, initially implemented by James Safranek in the *LOCO* software [5]. The reimplementation led to a software which was available online in the control room during the LHC injection tests and commissioning. *Aloha* is able to fit kick-response measurements and dispersion measurements. It has interactive access to the *MADX* model of the machine via a slim JAVA-API for *MADX*. Therefore a large variety of possible fit parameters is available.

Fitting procedure

A fit in *Aloha* varies a set of N_f parameters c_l, $1 \leq l \leq N_f$, of the model such that the differences between the measured and calculated observables are minimized. Concerning the analysis in this paper the observables are the elements of the response matrix R, whose elements are defined by

$$R_{ij} = \frac{u_i}{\delta_j}, \quad (1)$$

where u_i is the position (x or y) at the i^{th} monitor and δ_j is the kick of the j^{th} corrector. The difference between measurement and model is expressed by the difference vector $\vec{V}$ whose elements are defined by

$$V_k = R_{ij}^{\text{diff}} := \frac{R_{ij}^{\text{meas}} - R_{ij}^{\text{model}}}{\sigma i}. \quad (2)$$

R^{model} is the response matrix calculated from the model and R^{meas} is the measured one. σ_i denotes the rms noise of the i^{th} BPM. The fit minimizes the quadratic norm of V.

To approach the minimal solution the problem is linearized. As a first step the system of linear equations

$$S\Delta\vec{c} = \vec{V} \quad (3)$$

is solved in a least square sense to obtain a vector $\vec{c}$ representing the parameter changes. This is achieved with least square algorithms like SVD or MICADO. The sensity matrix S is defined by

$$S_{kl} = -\frac{\partial V_k}{\partial c_l} = \frac{1}{\sigma_i}\frac{\partial R_{ij}^{\text{model}}}{\partial c_l}. \quad (4)$$

These sensity-matrix elements are numerically approximated by the local fit gradient,

$$S_{kl} = \frac{R_{ij}^{\text{model}}(c_l + \delta c_l) - R_{ij}^{\text{model}}(c_l)}{\delta c_l \, \sigma_i} = \frac{\Delta R_{ij}(c_l)}{\sigma_i}. \quad (5)$$

The parameter increment δc_l has to be chosen carefully for each parameter. After determining $\Delta\vec{c}$ from Eq. (3) a new set of parameter-values can be calculated,

$$c_l{}' = c_l + \Delta c_l. \quad (6)$$

The values $c_l{}'$ are then applied to the model and the procedure is iterated until the parameters are stable.

To estimate the quality of a fit the rms of the difference of the response-matrix elements with respect to the monitor noise is used:

$$\Delta_{\text{rms}} = \sqrt{\frac{1}{N-1}\sum_{i,j} R_{ij}^{\text{diff}}\delta_j}. \quad (7)$$

R_{ij}^{diff} is defined in Eq. (2), δ_j is the kick of corrector j, N is the number of all valid elements of the response-matrix. This value will usually be larger than one and will converge to one when the fit error is of the same magnitude as the BPM noise. This would correspond to a perfect fit in our sense.

MODEL OF $\frac{\Delta p}{p}$ DEPENDENCE

The influence of systematic quadrupolar and sextupolar field errors in the main bends of the transfer line on the response matrix can be expressed by

$$\Delta R_{ij} = A_{ij}\left(\frac{\Delta K}{K} - \frac{\Delta p}{p}\right) + B_{ij}b_2 + C_{ij}b_3\frac{\Delta p}{p}. \quad (8)$$

$\frac{\Delta K}{K}$ denotes a systematic error of the main quadrupole strengths with respect to the nominal settings. b_2 and b_3 denote the systematic relative quadrupolar and sextupolar field errors in units of 10^{-4} with respect to the main field of the bend. These were implemented directly in the *MADX* model of the transfer line by the use of

$$k_{n-1} = \frac{b_n}{R_{\text{ref}}^{n-1}}\frac{\alpha}{l}10^{-4}(n-1)!, \quad (9)$$

where k_n denote the multipole strengths applied to the main bends in *MADX*, α is the bending angle of the magnet, l its length and R_{ref} is a reference radius which is defined for the main bends in the transfer line as $R_{\text{ref}} = 0.025$ m. The "true" momentum mismatch $\frac{\Delta p}{p}$ is given by

$$\frac{\Delta p}{p} = \frac{\delta p}{p} + \frac{\Delta p_0}{p}, \quad (10)$$

where $\frac{\delta p}{p}$ denotes the trimmed momentum offset and $\frac{\Delta p_0}{p}$ an a priori unknown initial momentum error.

There are four degrees of freedom which have to be determined by the fit algorithm: $\frac{\Delta p_0}{p}$, $\frac{\Delta K}{K}$, b_2 and b_3. The factors A_{ij}, B_{ij} and C_{ij} in Eq. (8) correspond to the fit gradients which are calculated implicitely from Eq. (5). B_{ij} and C_{ij} act with the same sign as A_{ij} in the horizontal plane and with the opposite sign than A_{ij} in the vertical one.

FIT RESULTS

A special fit method was implemented to combine the measurements with different momentum offsets $\frac{\delta p}{p}$ into one sensity matrix. This allowed to fit for all four parameters simultaneously, converging after 6 iterations to

$$\boxed{\begin{aligned} b_2 &= 0.85, & b_3 &= -5.06, \\ \frac{\Delta p_0}{p} &= 7.51 \times 10^{-4}, & \frac{\Delta K}{K} &= 5.61 \times 10^{-3}. \end{aligned}} \quad (11)$$

The fit error as defined by Eq. (7) results in $\Delta_{\text{rms}} = 1.99$, which is small compared to the initial values between 5 and 8 for the different measurements.

The b_3 was very well reproduced by various fit variants while the other three parameters can only be determined up to a constant ε since they are not completely decoupled. The fit procedure is insensitive to the transformation

$$\begin{aligned} \frac{\Delta p_0}{p} &\rightarrow \frac{\Delta p_0}{p} + \varepsilon, & \frac{\Delta K}{K} &\rightarrow \frac{\Delta K}{K} - \varepsilon, \\ b_2 &\rightarrow b_2 + \frac{2b_3}{R_{\text{ref}}}\langle D_x\rangle\,\varepsilon, & b_3 &\rightarrow b_3. \end{aligned} \quad (12)$$

Here $\langle D_x \rangle$ denotes the average horizontal dispersion over all the bends with errors.

Applying the values of Eq. (11) to the model results in a very good agreement between model and measurement as demonstrated in Fig. 4 and Fig. 5. The effect on the dispersion is not evident and has to be verified by further measurements.

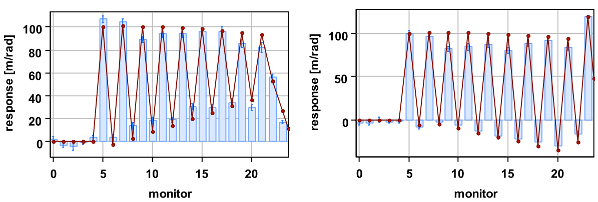

(a) $\frac{\delta p}{p} = -0.002$ (b) $\frac{\delta p}{p} = +0.002$

Figure 4: Horizontal response for the same corrector as in Fig. 2 with the values of Eq. (11) applied to the model. Bars represent the measured data, dots the updated model.

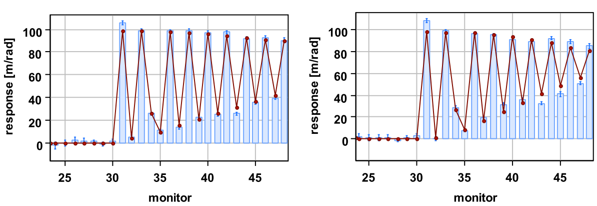

(a) $\frac{\delta p}{p} = -0.002$ (b) $\frac{\delta p}{p} = +0.002$

Figure 5: Vertical response for the same corrector as in Fig. 3 with the values of Eq. (11) applied to the model. Bars represent the measured data, dots the updated model.

CHROMATIC BEHAVIOUR

Figure 6 shows the dependence of the phase on $\frac{\delta p}{p}$ at the TI 8-LHC junction for the nominal model. The slope represents the natural chromaticity of the line which is similar for both planes and can be read from the plot as $Q'_x = -13.71$ and $Q'_y = -14.74$.

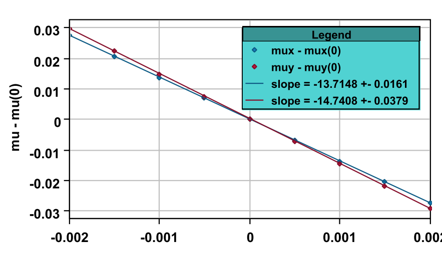

Figure 6: Chromaticity derived from the nominal model.

The influence of the b_2 and b_3 on the horizontal and vertical phases μ_x and μ_y is given by

$$\Delta\mu_x = Q'_x \left(\frac{\Delta p}{p} - \frac{\Delta K}{K} \right) + A_{2x} b_2 + A_{3x} b_3 \frac{\Delta p}{p}, \quad (13a)$$

$$\Delta\mu_y = Q'_y \left(\frac{\Delta p}{p} - \frac{\Delta K}{K} \right) - A_{2y} b_2 - A_{3y} b_3 \frac{\Delta p}{p}. \quad (13b)$$

A_{2x}, A_{2y}, A_{3x} and A_{3y} are positive factors which are calculated from the model. Therefore b_2 and b_3 act on the two planes with the opposite signs while the natural chromaticities (Q'_x, Q'_y), which are negative quantities, and $\frac{\Delta K}{K}$ act on both planes with the same sign.

Figure 7 shows the dependence of the phase for the model with the values of Eq. (11). The b_3 in the line approximately compensates the vertical natural chromaticity and results in a total vertical chromaticity of $\xi_y = +3.28$ and total horizontal chromaticity of $\xi_x = -34.11$ which is about twice the natural one. This explains the phase behavior already qualitatively demonstrated by Fig. 2 and Fig. 3.

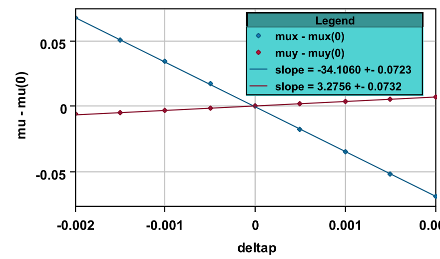

Figure 7: The chromaticity derived from the model with the values of Eq. (11).

SUMMARY AND OUTLOOK

Asymmetrical phase dependence on $\frac{\delta p}{p}$ was qualitatively observed for the two transverse planes in the TI 8 transfer line. By fits to several off-momentum kick response measurements clearly an unexpectedly high systematic sextupolar error (b_3) was identified (about 6 units of 10^{-4} at $R_{\text{ref}} = 25$ mm). From the resulting model the chromaticity of the line was extracted which explains very well the $\frac{\delta p}{p}$ dependence of the measured data. The natural chromaticity of the line is approximately compensated by the b_3 in the vertical plane and doubled in the horizontal plane. It is foreseen to repeat these off-momentum measurements with different time constants related to the ramp to check the nature of this b_3 (geometric or dynamic).

REFERENCES

[1] J. Wenninger, "Study of the TI 8 optics and beam stability based on beam trajectories", CERN AB-Note-2006-021 OP.

[2] M. Lamont et al., "the LHC Injection Tests", LHC Performance Note 001.

[3] I. Agapov et al., "TI 8 transfer line optics studies", LHC Performance Note 004.

[4] K. Fuchsberger, "Aloha - Optics studies by combined kick-response and dispersion fits", CERN BE-Note-2009-020 OP.

[5] J. Safranek, "Experimental Determination of Storage Ring Optics Using Orbit Response Measurements", Nucl. Instr. Meth. A, 388, 1997, p 27-36.